Molecular dynamics simulations of the Debye-Waller effect in shocked copper

William J. Murphy,* Andrew Higginbotham, and Justin S. Wark
Department of Physics, Clarendon Laboratory, University of Oxford, Parks Road, Oxford OX1 3PU, United Kingdom

Nigel Park
Material Modelling Group, AWE, Aldermaston, Reading, Berkshire RG7 4PR, United Kingdom
(Received 31 March 2008; published 23 July 2008)

We present an analysis of the directionally dependent x-ray structure factors (and, hence, intensities) predicted by nonequilibrium molecular dynamics simulations of statically compressed and shocked single crystals of copper, and comment on the feasibility of using experimentally measured intensities to infer temperature information. We further consider the behavior of the diffracted intensity from isentropically compressed samples.

DOI: 10.1103/PhysRevB.78.014109 PACS number(s): 61.05.cp, 62.50.Ef, 64.30.Ef

I. INTRODUCTION

The use of x-ray diffraction to interrogate the structure of shocked crystals on subnanosecond time scales is now a well-established technique, with recent experimental results providing some information on upper time limits necessary for plastic flow within various materials,[1] as well as on the underlying mechanisms of the widely studied shock-induced α-ϵ transition in laser-compressed single crystals of iron.[2] In parallel with the development of short-time-scale shock and diffraction experiments, the prediction of the response of matter to shock compression by means of nonequilibrium molecular dynamics (NEMD) simulations has been a burgeoning field, with a similar concentration of interest in shock-induced plasticity[3,4] and phase transitions.[5,6] With the rapid increase in computing power and storage over recent years, the length and time scale of such simulations are now starting to become directly comparable with those of the laser shock-compression experiments. The simulation of crystals with spatial dimensions of a reasonable fraction of a micron for durations of hundreds of picoseconds are now quite feasible, if not entirely routine. This convergence of scales has understandably led to direct comparisons being made between the x-ray diffraction patterns predicted by the NEMD simulations and those directly observed in experiments. For example, Bringa *et al.*[7] recently used NEMD simulations to calculate the shift in both the Bragg (reflected) and Laue (transmitted) peaks in shock-compressed copper. Their work provided information on the time-dependent shape of the unit cell of a sample of shocked copper, which in turn offers insight into plastic flow. Hawreliak *et al.*[8] directly compared the diffraction patterns predicted by NEMD with the experimental data for the α-ϵ transition in shocked iron, noting, among many other things, good agreement between the predicted x-ray linewidths in the ϵ phase and those seen experimentally—an observation which is consistent with the predicted mean size of two families of crystallites with orthogonal c axes.

However, while diffraction patterns have been simulated by use of NEMD calculations, to date an analysis of them has largely concentrated on the position or width of the diffraction peaks, rather than explicitly their intensity. The intensity of diffracted radiation associated with a particular Bragg peak (i.e., set of Miller indices) relative to the intensity diffracted from an uncompressed sample will be a function of the local structure factor of the crystal, and this structure factor can be significantly altered by the action of shock compression of the crystal. In particular, the reflectivity will alter both due to the shock-induced temperature rise and the compression. This temperature rise will influence the intensity of a particular reflection owing to the well-known Debye-Waller effect[9] as the increase in temperature results in a larger rms displacement of a particular atom around its mean position. However, the Debye-Waller factor is also a function of the effective Debye temperature Θ, and we note that under compression Θ will also change. For example, one might normally expect compression to steepen the potential, with a resultant increase in the effective Debye temperature, which will tend to reduce the rms displacement of the atoms. Such an increase in the effective Debye temperature would tend to increase the structure factor at finite temperatures; thus, the relative intensity of a particular Bragg reflection is not entirely trivial to calculate.

In this paper we present an initial analysis of NEMD calculations of the effect of shock compression on the expected intensities of Bragg reflections. We present the analysis in terms of effective Debye temperatures predicted by the NEMD for uniaxially compressed, hydrostatically compressed, and shock-compressed single crystals of copper, and compare these results with those predicted by analytic means. Given that the x-ray reflectivity is a function of temperature, we comment on the feasibility of using reflectivities as a temperature diagnostic of shocked crystals. Finally, as rapid isentropic compression is an area of great topical interest, we discuss the expected behavior of the relative x-ray intensities of crystals subject to such loading, noting that the x-ray reflectivity of higher diffraction orders can actually increase under these conditions.

II. DEBYE-WALLER FACTOR

In the absence of phase transitions (which we do not consider here), the main factor that will alter the relative intensity of the angularly integrated x-rays within a given peak will be the Debye-Waller factor, which is a function of both

the temperature T and the effective Debye temperature Θ. The overall intensity of a particular reflection is a function of many factors, including the degree of perfection of the crystal. For a perfect crystal we must use dynamical diffraction theory, whereas for completely imperfect crystals the kinematic approximation must be used.[10] In each case, however, the influence of a shock is twofold: first, the positions of the peaks are altered, as the change in lattice spacing results in a change in Bragg angle. For small one-dimensional compressions, the change in the position of a particular peak is given by a simple differentiation of Bragg's law,

$$\Delta\theta = -\tan\theta\frac{\Delta(2d)}{2d}, \tag{1}$$

where θ is the Bragg angle associated with the plane of spacing d. For large compressions, we must recalculate the angular position of the peak from the full form of Bragg's law; but in any case such a calculation is trivial and finding the location of a particular reflection in the case where compression occurs along all three orthogonal directions (for example, as a crystal changes from elastic toward hydrostatic conditions under shock compression) is also not difficult.

The intensity of the peak, however, will depend on the structure factor. Within the Debye-Waller theory, for a reciprocal lattice vector $\mathbf{G}$, the structure factor $S_{\mathbf{G}}^{T}$ at a temperature T, is given by

$$S_{\mathbf{G}}^{T} = S_{\mathbf{G}}^{0}\exp(-M), \tag{2}$$

where $S_{\mathbf{G}}^{0}$ is the structure factor for the perfect, unheated lattice, which is the sum over atoms at positions $\mathbf{r}_i$ of the atomic form factors f_i over all atoms in the unit cell,

$$S_{\mathbf{G}}^{0} = \sum_i f_i \exp(-i\mathbf{G}\cdot\mathbf{r}_i). \tag{3}$$

Note that for the compressions we consider here, there should be no change in the atomic form factor: we are not dealing with conditions such that pressure ionization occurs. The atomic form factor is, however, angularly dependent, and this should be taken into account when calculating real intensities. The temperature dependence enters into the factor M in Eq. (2). In the kinematic limit the intensity I of a particular reflection is proportional to the square of the structure factor, and thus,

$$I(T) = I(0)\exp(-2M), \tag{4}$$

where

$$2M = \frac{3h^2N_A|\mathbf{G}|^2}{mk_B\Theta}\left[\frac{T}{\Theta}\Phi\left(\frac{\Theta}{T}\right)+\frac{1}{4}\right], \tag{5}$$

and

$$\Phi(y) = \frac{1}{y}\int_0^y \frac{x}{e^x-1}dx. \tag{6}$$

T is the temperature in kelvin, h is Planck's constant, N_A is Avogadro's number, m is the atomic mass, and k_B is Boltzmann's constant. For the sake of brevity, as we are only presenting the simple Debye theory for reasons of illustration, we have assumed an isotropic solid, which is also valid for a cubic system due to the manner in which the resolved displacement is summed. In an anisotropically compressed crystal, there will be a directional dependence.

In the normal Debye theory the function $\Phi(y)$ takes into account that the phonon modes in the crystal are populated according to Bose–Einstein statistics, and the factor of 1/4 in Eq. (5) takes into account zero-point motion. Clearly in classical NEMD calculations such as those we present here, this is not appropriate, and the vibrational modes present within the simulation obey Boltzmann statistics. In the simulations in this paper we calculate the effect of compression and temperature on Bragg reflections by calculating the Fourier transform of the atomic coordinates provided by the NEMD simulations. Integration in reciprocal space around particular Bragg reflections provides a relative measure of the x-ray structure factor for the reflection in question, and the variation of this integral with reciprocal lattice vector for a particular temperature can be used to deduce an effective Debye temperature. As the NEMD simulations are classical, when quoting an effective Debye temperature, it will be related to the exponential falloff in integrated intensity by

$$2M = \frac{3h^2N_A|\mathbf{G}|^2}{mk_B\Theta}\left[\frac{T}{\Theta}\right]. \tag{7}$$

III. ANALYTIC CALCULATIONS

The main thrust of this paper is to use NEMD simulations as a tool to investigate how the intensity of x-rays diffracted by crystals is affected by temperature and compression. However, both as a comparison with NEMD simulations and as a tool in its own right, we can also use analytic models based on previously published forms of the Grüneisen parameter to predict the manner in which compression affects the Debye temperature. The Grüneisen parameter Γ used in the Grüneisen equation of state is defined as

$$\Gamma(V) = -\frac{\partial\ln\Theta}{\partial\ln V}, \tag{8}$$

and thus,

$$\frac{\Theta}{\Theta_0} = \exp\left(-\int_{V_0}^{V}\frac{\Gamma(V)}{V}dV\right), \tag{9}$$

where V is the volume.

We investigate four different forms of $\Gamma(V)$ for copper. The simplest model is to assume that Γ/V is constant.[11,12] More generally, the Grüneisen parameter can be expressed as a power of the volume. Pandya *et al.*[13] used a theoretical model based in perturbation theory taking into account terms due to the atomic orbitals of the material. Ramakrishnan *et al.*[14] gave an empirical result based on measuring how the temperature of a sample is affected by adiabatic pressure changes. The compressions used in that study were low compared with the regime normally probed by shock experiments. These three models can be summarized as all being of the form

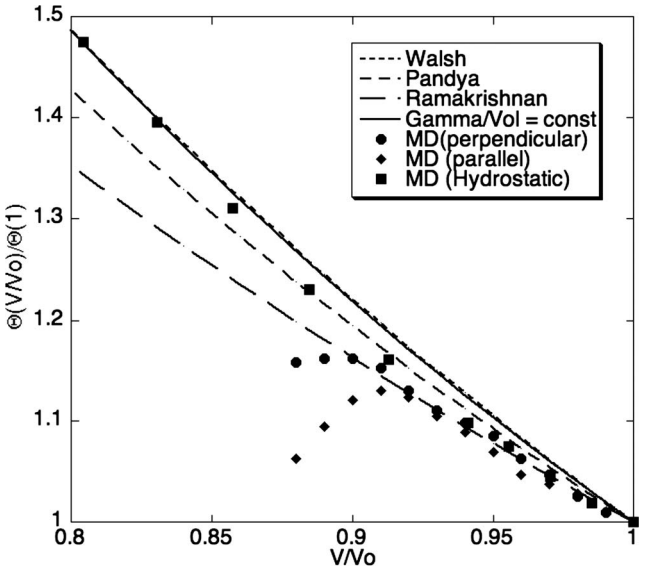

FIG. 1. Debye temperature as a function of compression calculated from MD and analytic models. The lines represent the analytic models from literature, and the points represent the results from MD simulations of the hydrostatic and uniaxial case (compressed along [001]). Results parallel and perpendicular to the compression direction are shown separately.

$$\Gamma(V) = \Gamma_0 \left(\frac{V}{V_o} \right)^q, \tag{10}$$

with the following values of Γ_0 and q for copper: ($\Gamma_0 = 1.98$, $q = 1.0$),[11,12] ($\Gamma_0 = 1.93$, $q = 1.085$),[13] and ($\Gamma_0 = 2.008$, $q = 1.33$).[14]

The fourth model which we shall consider is that provided by Walsh *et al.*,[15] who used experimental Hugoniot data in conjunction with the Mie–Grüneisen equation of state to deduce a polynomial fit for the Grüneisen parameter as a function of volume,

$$\Gamma(V) = \Gamma_0 + A\left(\frac{V_o}{V} - 1 \right) + B\left(\frac{V_o}{V} - 1 \right)^2 + C\left(\frac{V_o}{V} - 1 \right)^3, \tag{11}$$

where for copper they found $\Gamma_0 = 2.04$, $A = -3.296$, $B = 10.493$, and $C = -19.264$. We note that Walsh *et al.*[15] performed experiments on long time scales compared with the NEMD calculations, and the Hugoniot elastic limit (HEL) of copper was small compared with the pressures of interest; thus, their Grüneisen parameter corresponds to that which one might expect for close to hydrostatic compression of the lattice.

The four models for the Grüneisen parameter are used to predict the Debye temperature as a function of hydrostatic compression. All four are plotted alongside the NEMD hydrostatic and uniaxial compression data in Fig. 1, and we discuss how they compare with NEMD predictions in Sec. IV.

IV. MOLECULAR DYNAMICS CALCULATIONS

The intensity of x-rays scattered by a crystal (neglecting the effects of absorption and extinction) can be calculated from NEMD by taking the Fourier transform of the atomic coordinates at a particular moment in time. This gives the intensity in k space, $I(\mathbf{k})$,

$$I(\mathbf{k}) = \left| \sum_j \exp(-i\mathbf{k} \cdot \mathbf{r}_j) \right|^2, \tag{12}$$

where now the sum is over all of the atomic positions in the simulation. For a particular experimental geometry, the overall structure factor associated with a given incident x-ray with wave vector $\mathbf{k}_0$ and a scattered x-ray with wave vector $\mathbf{k}_s$ can be found by using $\mathbf{k} = \mathbf{k}_0 - \mathbf{k}_s$. Note that Eq. (12) is a sum over specific coordinates; thus, we have not explicitly taken into account the dependence of the atomic form factor on scattering angle, but as this is tabulated[16] it can also be included in explicit intensity calculations if necessary. While fast Fourier transform techniques can do this Fourier transform over the whole of the meaningful region of k space,[17] here we are only interested in the regions of intensity maxima surrounding specific Bragg reflections, and in this case it was computationally efficient to use a simple, rather than fast, Fourier transform. For all of the NEMD simulations presented here, the atomic coordinates were calculated using the MD code LAMMPS,[18] with the copper sample simulated using Mishin's EAM1 potential.[19]

A. Debye temperature: Uncompressed sample

In the simple Debye theory the Debye temperature itself is independent of temperature. As a first test of the predictions of the NEMD simulations, we calculated the Fourier transform of the atomic positions of an uncompressed sample at different temperatures and calculated the Debye temperature from the predicted x-ray reflectivities (i.e., from the relative integrated intensity of the Bragg peaks in reciprocal space). A $60 \times 60 \times 60$ conventional cell sample of copper with lattice parameter $a = 3.615$ Å was thermalized for 10 ps with periodic boundary conditions at temperatures T = 300, 600, 900, and 1200 K.

According to Eq. (5) we expect that the logarithm of the integrated intensity is proportional to $(-|\mathbf{G}|^2 T/\Theta^2)$. Thus, in Fig. 2 we plot the logarithm of the integrated intensity of the Bragg peaks as a function of $|\mathbf{G}|^2$ for a variety of temperatures, and the gradient of this line provides the Debye temperature. From this (Fig. 2) a value for the Debye temperature was calculated (see Table I). The average agrees well with literature values, indicating the applicability of the Mishin potential. The calculated Debye temperature decreases slightly as the temperature of the sample is increased. This is possibly due to the atoms exploring further into the anharmonic region of the potential as the temperature is increased.

B. Uniaxially compressed samples

To date NEMD simulations of the shock compression of single metal crystals predict elastic limits far higher than

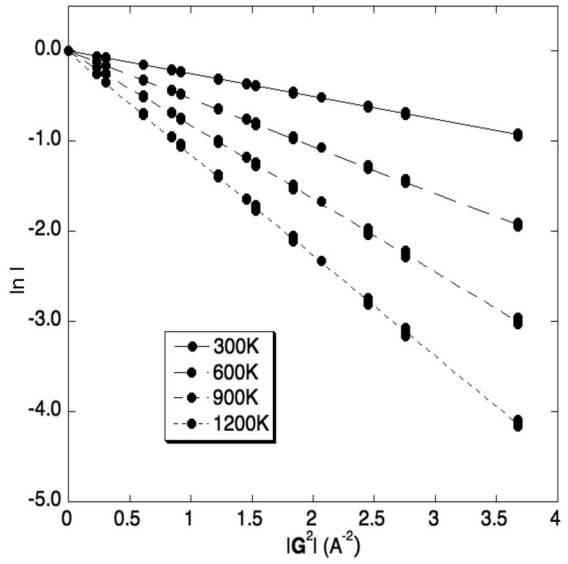

FIG. 2. MD simulations of the relative intensity of diffracted peaks as a function of reciprocal lattice vector for an uncompressed copper crystal.

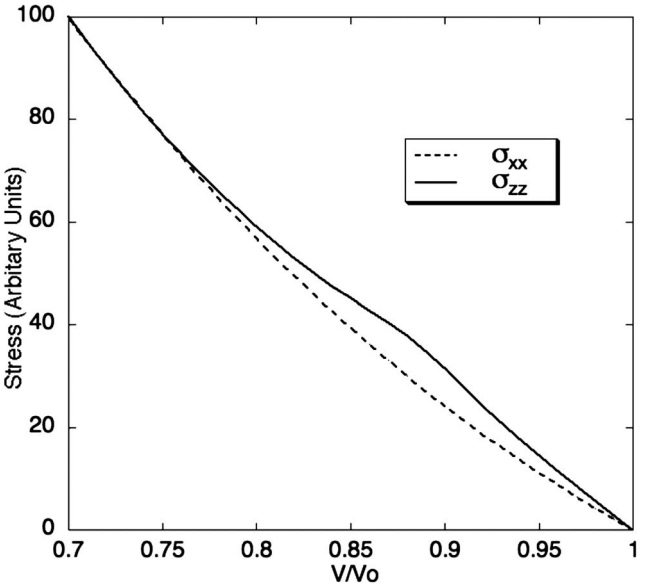

FIG. 3. Stress along the x axis (σ_{xx}) and the z axis (σ_{zz}) calculated from NEMD simulations of low-temperature Cu for compression along the [001] direction.

those seen in the majority of experiments. Indeed, the elastic limits are consistent with the theoretical limiting shear strength of a solid under compression and are typically up to 2 orders of magnitude higher than seen in long-time-scale (hundreds of nanoseconds) experiments. For example, in the work of Bringa *et al.*,[7] when a single crystal of copper simulated with the Mishin potential is shocked along the principal axis, completely elastic compression is seen up to compressions of order 15%, corresponding to pressures of order 350 kbar. While the addition of defects and a ramped pressure drive can somewhat reduce this value,[7] it is clear that at present NEMD simulations predict that very high elastic response can be observed on short time scales. We note also that for bcc crystals of iron, close to purely elastic response has been observed experimentally up to compressions of 6%,[20] in agreement with NEMD calculations.[21]

Thus, before simulating the change in intensities due to shock compression, in this section we consider how uniaxial elastic compression along a cube axis of a copper single crystal alters the calculated x-ray reflectivities. As in Sec. IV A, 864 000 atoms were taken, and for a variety of uniaxial compressions up to 12%, thermalized at 300 K. The crystal was compressed along the [001] axis, and the integrated reflectivities of Bragg spots in k space were calculated for the reflections corresponding to directions both along and perpendicular to the compression axis. From the variation of reflectivity with the square of the reciprocal lattice vector, a Debye temperature was again calculated. The Debye temperatures for the directions parallel and perpendicular to the compression are shown in Fig. 1, where they have been normalized to the Debye temperature for the uncompressed case discussed above. We note that, as expected with a steepening of the potential under compression, the Debye temperature increases roughly linearly under compression.

TABLE I. The Debye temperature calculated from samples thermalized at different temperatures.

T/K	Θ/K
300	322
600	321
900	316
1200	310
Average	317
Literature	315

It can be seen, however, that for compressions above about 9%, there is a radical change in the Debye temperatures. Above this point the Debye temperature reduces with compression along the compression direction, such that above 11% compression it is significantly lower in the compression direction than in the orthogonal direction. This is counterintuitive as one might expect that constraining the atoms in one direction would increase the effective Debye temperature for that direction.

This more complex behavior of the Debye temperatures is due to the effect of the Bain path. It is well known that uniaxial compression of a face-centered-cubic lattice along the [001] direction by a factor of $1/\sqrt{2}$ leads to a body-centered-cubic lattice, for which the shear stress must be zero. The stresses in the compression direction, σ_{zz}, and in the orthogonal direction, σ_{xx}, as a function of uniaxial compression along the z direction are shown in Fig. 3. These results were determined for a $10\times10\times10$ conventional unit cell sample simulation compressed in a canonical ensemble at 5×10^{-5} K to make temperature effects negligible and prevent shear relaxation by dislocations. As expected, the stresses are equal at the volume at which the lattice becomes body-centered-cubic. Between this point and zero compression, the stress in the compression direction is higher than that in the orthogonal direction, as expected. However, the

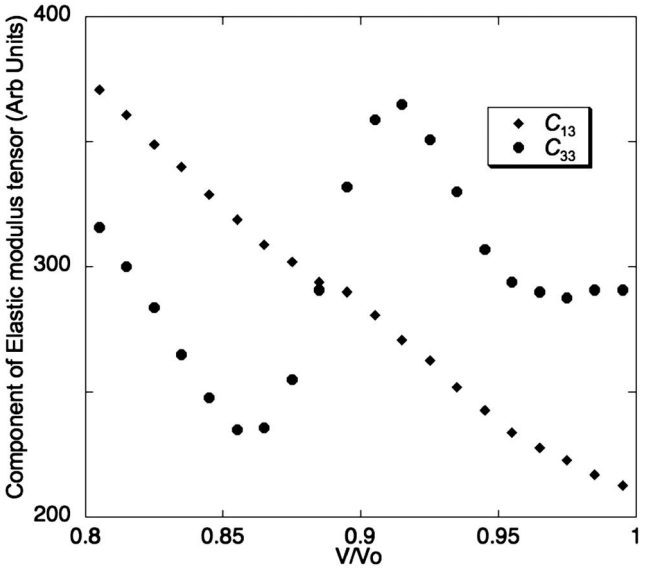

FIG. 4. C_{11} and C_{33} components of the elastic modulus tensor as a function of compression deduced from gradients of Fig. 3.

Mishin potential predicts that while the gradient of σ_{xx} increases monotonically with compression along the z direction, this is not the case for σ_{zz}. From these gradients we calculate the C_{13} and C_{33} components of the elastic modulus tensor. As cubic symmetry is lost on uniaxial compression, there are more than three independent terms in this tensor. In Fig. 4 we plot these elastic modulus terms as a function of uniaxial compression along z. It is evident that the maximum in the stiffness in the z direction occurs at the same compression as the maximum in the Debye temperature deduced from the integration of the intensities in k space.

C. Hydrostatically compressed samples

At high shock compressions of face-centered-cubic perfect single crystals, NEMD simulations predict the homogeneous generation of defects at the shock front, the motion of which can alleviate the shear stress. This results in the lattice tending toward the hydrostatic state, although the strength of the material may support some residual shear stress and prevent it from becoming completely hydrostatic. It should be noted that this remains an area of active interest: the mechanism of defect generation and motion has been predicted to be a function of the direction of shock compression. Compression of single crystals along the [001] direction activates a partial dislocation resulting in a stacking fault; in contrast compression along the [111] direction results in full dislocations via two partial loops.[22] In any case, for perfect crystals the elastic limit is extremely high compared with values found experimentally on longer time scales. As noted in Sec. IV B, Bringa *et al.*[7] showed that pre-existing defects can reduce the effective elastic limit, although no simulation has yet been performed that reproduces the comparatively low elastic limits seen in long-time-scale experiments.

However, in any case the generation and motion of the defects acts so as to remove the shear stress, and the lattice which is initially tetragonal with a large aspect ratio under elastic compression tends more toward a compressed cube as the shear stress is released and the hydrostat approached.[23] It is thus of interest to use the NEMD simulations to calculate the effective x-ray Debye temperatures for hydrostatically compressed samples. These Debye temperatures, deduced by identical means to those outlined in Sec. IV A, are shown alongside analytically fitted Grüneisen parameters in Fig. 1. It can be seen that these more closely follow the higher compression Grüneisen parameter predictions, and reasonable agreement with the analytic model based on experimental data of Walsh *et al.*[15] is seen for larger compressions.

D. Shock-compressed samples

Under shock compression we not only expect the Debye temperature to change, but we also expect a rise in temperature. We stress that as these simulations have been performed with shock compression of a perfect copper crystal along the [001] axis, stacking faults are not generated at the shock front until compressions in excess of 15%.

The simulated sample was a $30\times30\times130$ conventional cell crystal oriented with the principal axis along x, y, and z with periodic boundary conditions in the x and y directions and shrink wrapped boundary in the z direction. This was thermalized to 293 K to match the experimental parameters of Walsh *et al.*[15] To generate the shock all atoms within five lattice parameters of $z=0$ were fixed together and then driven as a unit into the crystal in the positive z direction at the desired shock speed ($U_p=108$, 181, 362, 542, 651, 687, and 723 ms^{-1}). A $30\times30\times30$ conventional unit cell section situated 80 conventional cells behind the shock front when it reached the other end of the crystal was used to calculate the corresponding reciprocal space intensity.

We note that the samples considered here, which were initially thermalized to room temperature, predict an increase in the diffracted intensity for higher-order reflections for low shock compressions. Only once we reach compressions of between 7% and 10% do we start to observe a decrease in the diffracted intensity. Physically this corresponds to the constraining of the atoms by the increased steepness of the potential under compression being more important than any temperature rise associated with the compression. As the Hugoniot for a weak shock lies very close to the isentrope, we shall return to this point when we discuss isentropic compression in Sec. V.

The data of Walsh *et al.*[15] described in Sec. III can also be used to predict the change in intensity under shock compression, as Walsh *et al.* also used the experimental data to predict the temperature rise as a function of shock compression, as well as the compression-dependent Grüneisen parameter. The falloff in diffracted intensity as a function of the relative volume according to the data of Walsh *et al.* is shown for copper in Fig. 5, alongside the NEMD predictions. It can be seen that the model of Walsh *et al.* exhibits qualitatively the same response as the NEMD shock simulations.

Shocking the sample to a point above the Hugoniot elastic limit generated a large number of dislocations. These have the effect of broadening the peaks in reciprocal space, particularly the higher-order peaks (see Fig. 6). To calculate the

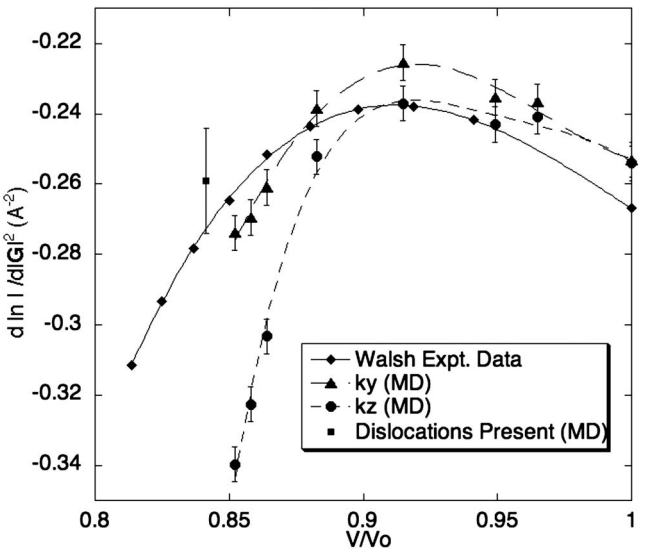

FIG. 5. Exponent of the Debye-Waller factor per reciprocal vector squared ($-2M/|\mathbf{G}|^2$) for copper shocked to V/V_o times its original volume, calculated from MD simulations of single crystals shocked along the principle axis and from data of Walsh *et al.* (Ref. 15).

intensity in reciprocal space, a 1.9×10^6 atom block was taken from the shocked region and the Fourier transform of the atomic coordinates calculated. Integrating over the resultant Bragg peaks and subtracting the background gives a result close to the prediction based on the figures of Walsh *et al.*[15] (the data point labeled "Dislocations Present" in Fig. 5). Due to the relaxation of the shear stress by the generation and motion of the dislocations, there is no noticeable directional dependence in the Debye-Waller factor within the error bars.

E. Strong-shock limit

In the strong-shock regime, where the velocity of the plastic wave exceeds that of the elastic wave it is usually found

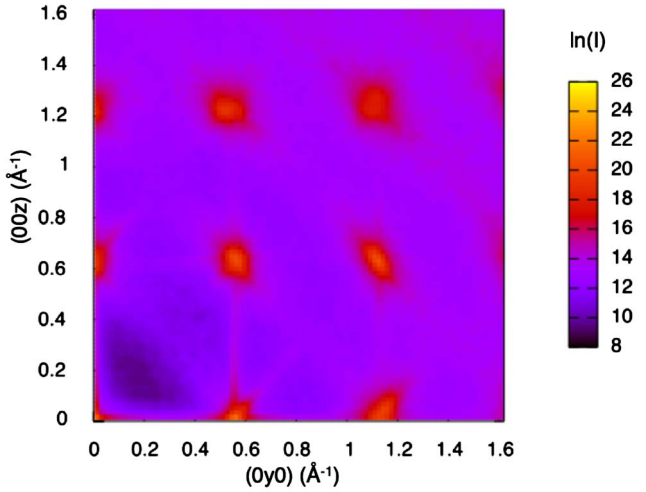

FIG. 6. (Color online) Intensity in the plane in k space corresponding to the [100] plane intersecting with the origin for a MD simulation of a shock in the [001] direction to above the Hugoniot elastic limit (HEL).

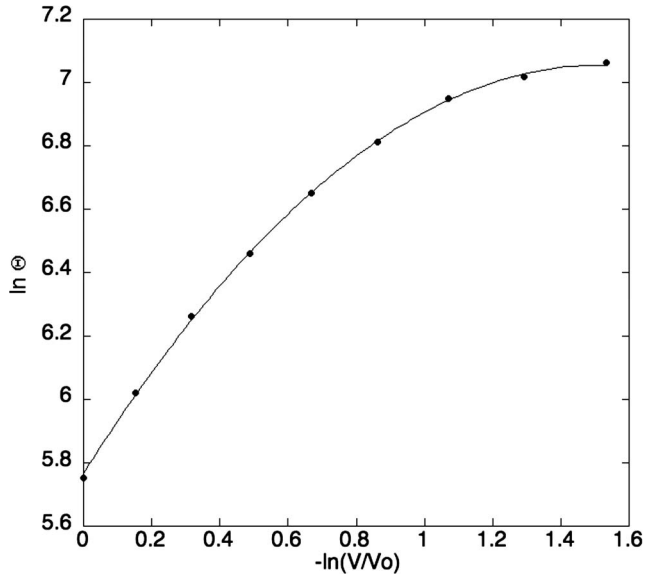

FIG. 7. Log-log plot of Debye temperature vs compression for MD simulated copper sample compressed hydrostatically fitted with a polynomial. The gradient gives the Grüneisen parameter.

that the shock speed U_s is related to the particle velocity U_p by

$$U_s = C_0 + s_1 U_p, \tag{13}$$

where s_1 is a constant and C_0 is close to the bulk sound speed. It can be shown that the Grüneisen parameter is a function of the volumetric compressive strain, $\epsilon=1-V/V_0$, and s_1, such that in the limit of $\epsilon=0$, $\Gamma=2s_1-1$.[23,24] Furthermore, the observation that s_1 is a constant for strong shocks implies that there is a limit to the compression,[25] $\epsilon=1/s_1$, and that at this limiting compression $\Gamma=2(s_1-1)$. Therefore at the limiting compression under shock conditions, the Grüneisen parameter is exactly 1 less than under ambient conditions.

In order to test how well the Debye temperatures deduced from the NEMD obey the above relations, we plotted Θ as a function of hydrostatic compression, as shown in Fig. 7. The atomic coordinates were generated by setting up an ideal $60\times60\times60$ conventional cell crystal already compressed by decreasing the lattice parameter and then thermalizing this to 300 K.

The data were fitted with a polynomial

$$\ln(\Theta) = A[-\ln(V/V_0)]^2 + B[-\ln(V/V_0)] + C, \tag{14}$$

which yielded the coefficients $A=-0.56\pm0.01$, $B=1.71\pm0.03$, and $C=5.76\pm0.02$. This upon differentiation yields

$$\Gamma = -\frac{d\ln(\Theta)}{d\ln(V/V_0)} = -2A\ln(V/V_0) + B. \tag{15}$$

Thus, for $\epsilon=0$, we deduce $\Gamma=1.71\pm0.03$, which we note is in reasonable agreement with the analytic Grüneisen coefficients discussed in Sec. III, and experiments give a value of $s_1=1.489$,[23] which implies $\Gamma=1.98$. This experimental value of s_1 implies a limiting compression of 0.67. If we solve Eq.

(15) for $\Gamma=0.71$, i.e., 1 less than the value under ambient conditions, we deduce a limiting compression of 0.59 ± 0.03, which is lower than the experimental figure, but it should be noted that this is a very high compression, and we would not necessarily expect the potential used in the NEMD to be valid at the high shock pressures necessary to asymptote toward this value.

V. ISENTROPIC COMPRESSION

The possibility of compressing a crystal along an isentrope, via ramped compression, has attracted considerable attention in recent years,[26,27] as such a technique may allow the creation of solid state matter at compressions far in excess of those achievable in diamond anvil cells.

Given the growing interest in isentropic compression on short time scales and the stated desire by some workers to diagnose the lattice compressed in such a way via x-ray diffraction, it is clearly of relevance to explore how we would expect the Debye-Waller factor to behave under such conditions. In this section we show that very simple considerations indicate that for a sample compressed at finite temperature, we would actually expect an increase in the intensity of the higher-order diffraction peaks.

Let us consider a simple model of a solid, where we take the Grüneisen parameter to be constant. In such a model

$$\frac{\Theta}{\Theta_0}=\left(\frac{V}{V_0}\right)^{-\Gamma}, \tag{16}$$

and along an isentrope

$$\frac{T}{T_0}=\left(\frac{V}{V_0}\right)^{-\Gamma}. \tag{17}$$

If $\mathbf{G}_0$ is the reciprocal lattice vector of a particular reflection under ambient conditions, then $\mathbf{G}=\mathbf{G}_0(V/V_0)^{-1/3}$ for hydrostatic compression. Now the exponent in the Debye-Waller factor M scales as

$$M\propto\frac{|\mathbf{G}|^2T}{\Theta^2}\propto\frac{|\mathbf{G}_0|^2T_0}{\Theta_0^2}\left(\frac{V}{V_0}\right)^{[\Gamma-2/3]}, \tag{18}$$

and thus

$$\frac{M}{M_0}=\left(\frac{V}{V_0}\right)^{[\Gamma-2/3]}. \tag{19}$$

Thus, as $\Gamma>2/3$, we find that M decreases under compression, and as the intensity of a Bragg peak is proportional to $\exp(-2M)$ in the kinematic limit, at finite temperatures we expect an increase in diffracted intensity under isentropic compression.

The physical reason for this increase in reflectivity is that under isentropic compression the increase in the stiffness of the lattice is a more important effect than the temperature rise. For, although the thermal energy of an atom is increased, the rms amplitude of its vibration not only decreases in absolute terms, but, importantly for the intensity of diffracted radiation, actually decreases as a fraction of the lattice spacing even though the lattice is being compressed. For small compressions the shock adiabat lies close to the isentrope, and thus we would expect that for small shock compressions, starting at finite temperature, there is actually an increase in the reflectivity of higher-order reflections. For the case of copper here, only once the compression due to the shock exceeds ~10% does the increase in temperature start to dominate over the increased strength of the lattice and the structure factor start to decrease. This effect can also be seen in Fig. 5.

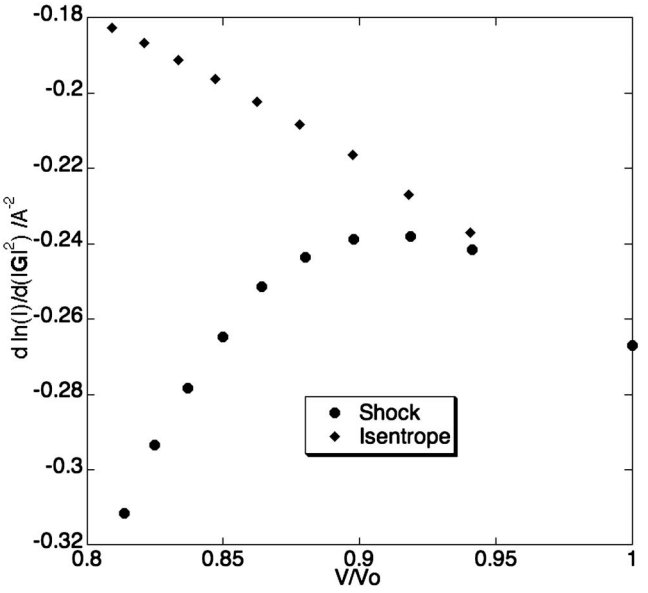

FIG. 8. Exponent of Debye-Waller factor per reciprocal vector squared for copper compressed via shock compression (circles) and isentropic compression (squares). Values are calculated from data of Walsh *et al.* (Ref. 15).

Walsh *et al.*[15] used a Mie–Grüneisen equation of state to calculate isentropic figures for temperature and compression. By using these, the Debye temperature can be calculated and the Debye-Waller factor deduced (see Fig. 8). These agree with our prediction that the intensity of the diffracted signal increases the more the material is compressed isentropically.

VI. RELATION TO EXPERIMENTS

Given that x-ray diffraction experiments on picosecond and nanosecond time scales are currently being performed, it is useful to consider to what degree the effects discussed above may be observable experimentally. Our analysis has concentrated on the degree to which the Debye-Waller factor is altered by shock compression, insomuch that the temperature of the lattice changes, but so also does its effective Debye temperature. As the Debye-Waller factor M is proportional to the square of the reciprocal lattice vector, it is evident that the effects will be most apparent for high-order reflections, which in turn require high-energy, short-wavelength x-rays in order to be observed.

In the field of laser-plasma interactions, where much of the work on time-resolved diffraction from shocked samples is being performed, x-rays of durations ranging from a few tens of picoseconds to several nanoseconds can be produced

by focusing high power optical radiation to intensities of order $10^{14}-10^{16}$ W cm^{-2} onto solid targets. In such experiments, the x-rays are emitted from transitions within highly ionized atoms; and typically in the past the resonance line of helium-like ions has been used. Given the laser energies and intensities available with the systems that have been used for shock compression and diffraction experiments, the highest photon energies used to date correspond to the helium resonance line of copper at 8.4 keV (although it has been shown that this could be extended to the resonance line of He-like Ge).[28]

On the other hand, in the picosecond and subpicosecond regime, the huge intensities that can be produced $>10^{18}$ W cm^{-2} induce the excitation and breaking of plasma waves, resulting in short bursts of energetic electrons penetrating the underlying target, producing a short burst of $K\alpha$ emission in an analogous manner to a conventional x-ray tube. It has been shown that such techniques can readily produce *K*-shell radiation up to 22 keV.[29] With such radiation sources, in principle at least, it should be possible to record reflections from copper crystals with Miller indices up to $\sqrt{h^2+k^2+l^2}$ of order 12. For an unshocked sample at room temperature, assuming a Debye temperature of 315 K, we would expect the intensity of such orders to be 2.8% of the (002) reflections (taking into account the dependence of the atomic form factor on scattering angle). If copper was shocked to 0.8 times its original volume, the ratio of the (579) to the (002) peak would be almost 2.5 times less than would be expected for the uncompressed sample at room temperature.

For the case of distinguishing between isentropic and shock compression the figures are even more promising. Consider copper compressed to 0.8 times its original volume. If it is compressed isentropically, the ratio of the (579) peak to the (002) peak will be more than ten times larger than if it is shocked to the same compression.

It is clear that the temperature affects the intensity of the diffraction patterns markedly. The problem lies in separating this effect from the compression effect. The compression itself can be measured readily from the peak shift but the limiting factor is deducing what effect this has on the Debye temperature.

VII. SUMMARY

The effect of temperature on the diffraction pattern of a shocked sample has been investigated through the use of NEMD and also by examining empirical and theoretical fits to the Grüneisen parameter from literature values. These two approaches give qualitatively similar results. It is apparent that the temperature has a significant effect on the intensity of the diffracted peak. However the effect is complicated by the effect of compression. This means that the Debye-Waller factor gives the combined effect of the temperature and Debye temperature. In order to isolate the temperature, the Debye temperature must first be deduced and this requires an accurate form for the Grüneisen parameter. Even without this parameter, the combined effect gives a figure for (T/Θ^2) which in itself may be interesting.

ACKNOWLEDGMENTS

The authors gratefully acknowledge financial support from a number of organizations. W.J.M. is grateful for support from AWE Aldermaston. A.H. has been generously supported by Daresbury Laboratory under the auspices of the NorthWest Science Fund.

*william.murphy@physics.ox.ac.uk

[1] K. Rosolankova, J. S. Wark, E. M. Bringa, and J. Hawreliak, J. Phys.: Condens. Matter **18**, 6749 (2006).
[2] D. H. Kalantar *et al.*, Phys. Rev. Lett. **95**, 075502 (2005).
[3] Y. M. Gupta, J. Appl. Phys. **48**, 5067 (1977).
[4] B. L. Holian and P. Lomdahl, Science **280**, 2085 (1998).
[5] K. Kadau, T. C. Germann, P. S. Lomdahl, and B. L. Holian, Science **296**, 1681 (2002).
[6] K. Kadau, T. C. Germann, P. S. Lomdahl, R. C. Albers, J. S. Wark, A. Higginbotham, and B. L. Holian, Phys. Rev. Lett. **98**, 135701 (2007).
[7] E. M. Bringa, K. Rosolankova, R. E. Rudd, B. A. Remington, J. S. Wark, M. Duchaineau, D. H. Kalantar, J. Hawreliak, and J. Belak, Nat. Mater. **5**, 805 (2006).
[8] J. Hawreliak *et al.*, Phys. Rev. B **74**, 184107 (2006).
[9] P. Debye, Ann. Phys. **43**, 49 (1914).
[10] W. H. Zachariasen, *Theory of X-Ray Diffraction in Crystals* (Dover, New York, 2004).
[11] Z. H. Fang and L. R. Chen, J. Phys.: Condens. Matter **6**, 6937 (1994).
[12] H. Schlosser, P. Vinet, and J. Ferrante, Phys. Rev. B **40**, 5929 (1989).
[13] C. V. Pandya, P. R. Vyas, T. C. Pandya, and V. B. Gohel, Bull. Mater. Sci. **25**, 63 (2002).
[14] J. Ramakrishnan, R. Boehler, G. H. Higgins, and G. C. Kennedy, J. Geophys. Res. **83**, 3535 (1978).
[15] J. M. Walsh, M. H. Rice, R. G. McQueen, and F. L. Yarger, Phys. Rev. **108**, 196 (1957).
[16] J. Ibers and W. C. Hamilton, *International Tables for X-Ray Crystallography* (Kynoch, Birmingham, UK, 1974), Vol. IV.
[17] G. Kimminau, B. Nagler, A. Higginbotham, W. Murphy, J. Wark, N. Park, J. Hawreliak, D. Kalantar, H. Lorenzana, and B. Remington, AIP Conf. Proc., Hawaii, 2007, Vol. 955, p. 1251.
[18] S. Plimpton, J. Comput. Phys. **117**, 1 (1995).
[19] Y. Mishin, M. J. Mehl, D. A. Papaconstantopoulos, A. F. Voter, and J. D. Kress, Phys. Rev. B **63**, 224106 (2001).
[20] D. H. Kalantar *et al.*, Rev. Sci. Instrum. **74**, 1929 (2003).
[21] K. Kadau, T. C. Germann, P. S. Lomdahl, and B. L. Holian, Phys. Rev. B **72**, 064120 (2005).
[22] T. C. Germann, B. L. Holian, P. S. Lomdahl, and R. Ravelo, Phys. Rev. Lett. **84**, 5351 (2000).
[23] E. M. Bringa, J. U. Cazamias, P. Erhart, J. Stölken, N. Tanushev, B. D. Wirth, R. E. Rudd, and M. J. Caturla, J. Appl. Phys. **96**, 3793 (2004).

[24] D. S. Drumheller, *Introduction to Wave Propagation in Nonlinear Fluids and Solids* (Cambridge University Press, Cambridge, 1998).
[25] M. A. Meyers, *Dynamic Behavior of Materials* (University of California, Berkeley, 1994).
[26] R. F. Smith, S. M. Pollaine, S. J. Moon, K. T. Lorenz, P. M. Celliers, J. H. Eggert, H. S. Park, and G. W. Collins, Phys. Plasmas **14**, 057105 (2007).
[27] D. B. Reisman, A. Toor, R. C. Cauble, C. A. Hall, J. R. Asay, M. D. Knudson, and M. D. Furnish, J. Appl. Phys. **89**, 1625 (2001).
[28] K. B. Fournier, M. Tobin, J. F. Poco, K. Bradley, S. B. Hansen, C. A. Coverdale, D. Beutler, M. Severson, E. A. Smith, and D. L. Reeder, J. Phys. IV **133**, 449 (2006).
[29] H. S. Park *et al.*, Phys. Plasmas **13**, 056309 (2006).